# Merocyanine 540 as an Optical Probe of Transmembrane Electrical Activity in the Heart

Abstract. *Frog hearts stained with merocyanine 540 show a 1.5 to 2.0 percent increase in fluorescence intensity at 585 nanometers during the cardiac action potential when excited with a 540-nanometer light beam. Fluorometric action potentials similar to those recorded with intracellular microelectrodes in pacemaker, atrial, and ventricular tissues were recorded by focusing a 1-millimeter excitation beam on various regions of the heart. The signal-to-noise ratio for a single action potential ranged between 10/1 and 40/1. In spontaneously pacing hearts the slower rate of rise of the fluorescence action potential is due to the slow propagation of the electrical signal. In solutions containing normal calcium concentrations the fluorometric signal is altered by contractions. Merocyanine 540 is biologically inert as it stains the cardiac cell membrane and acts as a sensitive optical probe of the change in transmembrane potential.*

In giant squid axon, 180 dyes have been shown to alter their fluorescence intensity in response to changes in membrane potential (*1, 2*). Of the dyes that exhibit an optical response in the giant squid axon, merocyanine 540 is one of the more sensitive probes. With peak excitation and fluorescence at 575 and 585 nm, respectively, the fluorescence increases by 0.1 percent over the background fluorescence when the membrane is depolarized by 100 mv. Studies with cyanine dyes (*3, 4*) bound to red blood cells also demonstrated emission dependent on membrane potential. In the experiments described here merocyanine 540 was used to determine its effectiveness as an optical probe in heart muscle.

The heart of the bullfrog *Rana catesbeiana* was removed and washed in Ringer solution containing 116 m*M* NaCl, 3 m*M* KCl, 2 m*M* $NaHCO_3$, and 1 m*M* $CaCl_2$. Either the atrium, the ventricle, or the whole heart was stretched and sutured to a stainless steel ring (2.0 cm in diameter) containing a tension transducer (Micro Measurements EA 09 015 DJ-120 microstrain gauge). The preparation was incubated for 5 to 15 minutes in Ringer solution containing $10^{-5}$ to $10^{-4}$*M* merocyanine 540 (Eastman Organic Chemicals), and excess dye was then thoroughly washed out. Isometric tension was monitored routinely to confirm that the staining procedure did not injure the muscle.

The heart was then immobilized at the center of a Lexan chamber, permitting the simultaneous recording of the fluorescence and absorption of the tissue. Light from a water-cooled 45-watt tungsten-halogen lamp (Westinghouse 6.6 T 242/Q/Cl) was collimated, passed through a narrow-bandwidth 540-nm interference filter (Baird Atomic), and focused on the muscle. This arrangement provided 1 to 10 $\mu w/mm^2$ of quasi-monochromatic light at 540 nm. The transmitted light was collected and focused on the surface of a photodiode (EG & G Inc. PV 444), while the fluorescent light (forward emission) was collected, passed through a 580- to 650-nm interference filter, and focused on another photodiode (the response time of the system was 1 khz). Care was exercised to prevent the reflected light from entering the photodiode by altering the angle of incidence of the excitation beam. For spectral measurements, the interference filters were replaced by monochromators (Bausch & Lomb grating monochromator 33-86-48).

Figure 1A shows the time course of the scattered light from an unstained muscle (top trace) during contraction (lower trace). In the presence of 1 m*M* $Ca^{2+}$, the mechanical motion of the heart produces a change in the intensity of scattered light of approximately 5 percent. After the muscle is stained with merocyanine 540, the mechanical motion of the heart results in even larger artifacts being superimposed on the optical signal of the dye (Fig. 1B). The shape, amplitude, and direction of the signal depend on the area of the muscle being sampled for fluorometry. In Fig. 1C, contraction is completely suppressed, and the fluorescence signal takes the characteristic shape of a cardiac action potential, with a fast upstroke, prominent plateau, and slow repolarization.

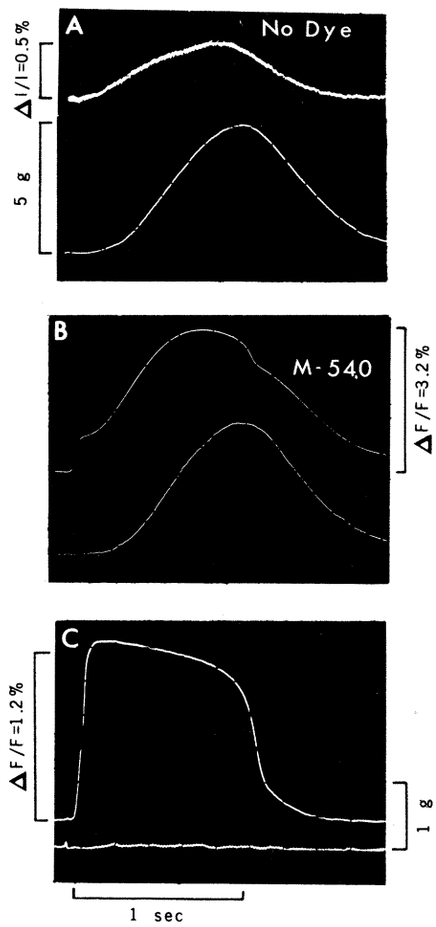


Fig. 1. Effect of contraction on the optical response of a merocyanine-stained frog ventricle. (A) The 585-nm scattered light of an unstained ventricle is monitored. The tension generated during contraction (lower trace) causes an increase of 0.5 percent in the scattered light (top trace). (B) The muscle is stained with merocyanine 540 and the calcium concentration of the bathing solution is kept at 1 m*M*. The optical signal (top trace) increases (1.2 percent) before any significant tension develops, but the fluorescence signal is then altered as the muscle contracts. (C) Contraction is completely suppressed by prolonged perfusion in $Ca^{2+}$-free solution (lower trace) and the fluorescence increase of 1.2 percent (top trace) has the characteristic time course of the ventricular action potential.

In Fig. 2, the fluorescence from a 2-mm incident light spot is monitored simultaneously with a continuous recording of a membrane potential with a microelectrode impaled in one of the cells within the area of the light beam. The muscle is stained and exposed to a Ringer solution containing 50 $\mu M$ $Ca^{2+}$ for 20 minutes, which suppresses the motion artifact. Comparison of the fluorometric ($V_f$) and microelectrode ($V_e$) traces in a spontaneously pacing ventricle shows remarkable similarity in the time course of the two traces (Fig. 2, A and B). However, small differences in the time course, especially in the onset of the rate of rise of the upstroke of the action potential, were often recorded. The rise time of the microelectrode is faster (15 msec) than that of the fluorescence action potential (40 msec, Fig. 2C). The discrepancy between the two rise times is partly due to the conduction delay that occurs as the electrical signals invade the 2 mm of tissue exposed to the light beam [action potential propagates at 0.1 m/sec at 20°C (*5*)]. Consistent with such an assertion, the rise time of the optical action potential becomes more rapid with smaller excitation light beams or with massive electrical stimulation of the ventricle (see Fig. 3A).

Small excitation beams make it possible to scan for the shape and the amplitude of the electrical signal at various parts of the heart. Figure 3 shows the fluorometric recording of action potential in ventricular (A), atrial (B), and sinus venosus (C) regions of the same heart. The charac-

teristic differences in duration and shape of the action potential and the resting potential previously observed in microelectrode studies (*5*) can be clearly seen fluorometrically. When a 1-mm-diameter beam is focused on the pacemaker region, a 0.25-mm displacement of the beam is sufficient to lose the pacemaking activity. The size of the incident beam is the limiting factor in the spatial resolution of the signal. The average fluorescence emission from the atrium is 20 to 40 percent higher than that from the ventricle. This is partly due to the higher optical density of the ventricle, caused by the presence of oxymyoglobin, which absorbs strongly at 544 and 581 nm (*6*).

Physiological interventions such as increasing the frequency of stimulation shortened the action potential, and cooling prolonged the fluorometrically measured action potential, confirming the results obtained with intracellular recordings. Pharmacological intervention (addition of epinephrine) or ionic intervention (addition of $Ni^{2+}$ or $Mn^{2+}$) produced characteristic changes in the fluorometric action potential similar to those recorded with intracellular electrodes. These results suggest that merocyanine 540 fluorescence monitors the changes of transmembrane potential without interacting significantly with pharmacological or ionic agents to qualitatively alter the optical signal.

In atria stained with merocyanine 540, the corrected absorption spectrum shows a 540-nm peak and a prominent shoulder at 570 nm. The generation of an action potential results in a 0.1 to 1.0 percent decrease in absorption at 540 nm and a 0.1 to 0.5 percent increase at 575 nm. These optical absorption signals at 540 and 575 nm are in opposite directions, but their time course is similar to that of the fluorescence action potentials. These results qualitatively resemble those obtained with squid axon (*7*), although the optimum signal in the axon is obtained through the absorption measurements at 570 nm rather than through the fluorescence (probably because of the high optical density of the myocardium). In the present experiments with either 540- or 570-nm excitation beams, the fluorescence emission in the heart peaks at 585 nm, compared to 610 nm in giant axon (*8*). However, the cardiac action potential, recorded as an increase in fluorescence intensity, is an order of magnitude larger with the 540-nm than with the 575-nm excitation beam. The discrepancy between these results and those reported for the nerve (*7*) may be due to the use of Pluronic F-127 (BASF Wyandotte Corporation) as a solvent for merocyanine 540 in seawater. In fact, in experiments where 0.2 percent Pluronic was used to dissolve higher concentrations of the dye in Ringer solution, the major absorption peak shifted from 540 to 570 nm and the amplitude of the fluorescence optical signal measured with a 570-nm excitation beam became equivalent to that measured with a 540-nm beam. In the heart the selective enhancement of the 570-nm absorption by Pluronic suggests that the 540- and 570-nm bands may represent two separate binding sites. Alternatively, Pluronic may increase the concentration of dye molecules in a state in which they absorb light at 570 nm. This is consistent with the transition from dimer to monomer postulated by Ross *et al.* (*7*) as the mechanism responsible for the optical behavior of merocyanines in nerve tissue.

The photodynamic effect of merocyanine 540 (*2*) consistently observed in nervous tissue (*9, 10*) seems to be absent or insignificant in heart tissue. In fact, 2 to 5 hours of exposure of merocyanine-stained hearts to beams of varying diameters (0.1 to 1.0 cm) and light intensities seems to have either little or no effect on the viability of the preparation. Although in the experiments illustrated in Figs. 1 to 3 we used preparations bathed in air-equilibrated Ringer solution, in experiments where the Ringer solution was saturated

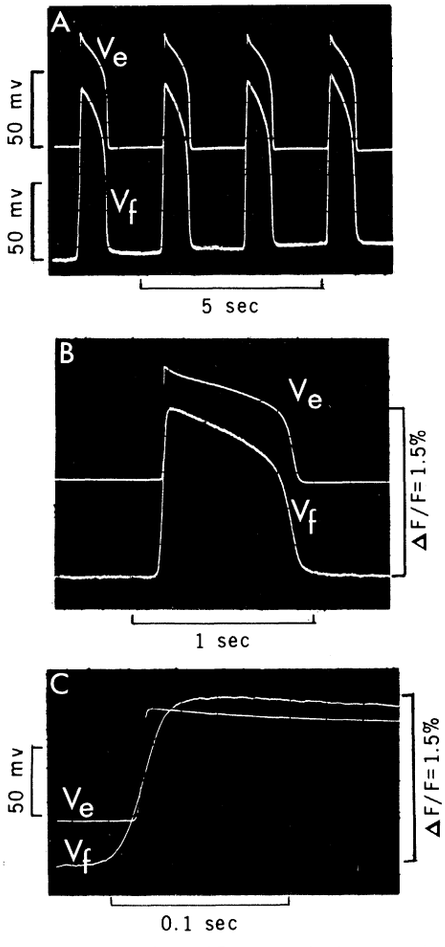


Fig. 2. Comparison of fluorometric electro-optical response with intracellularly recorded action potentials. Frog ventricular flap is stained with merocyanine 540 and is equilibrated in 50 $\mu M$ calcium Ringer solution to suppress the contraction. (A) Four spontaneous action potentials are recorded with a microelectrode (trace $V_e$) impaled in one of the cells excited with the 2-mm incident light beam. The simultaneously recorded fluorescence signal is shown in the lower trace ($V_f$). The fluorescence signal increases transiently by 1.8 percent as the membrane depolarizes and follows a time course similar to that of the action potential recorded with the microelectrode ($V_e$). (B) The time course of the plateau and repolarization are fairly similar but (C) the upstroke of the fluorometric action potential ($V_f$) is always slower than that recorded with the microelectrode ($V_e$). For $V_f$, 50 mv = 1.2 nw.

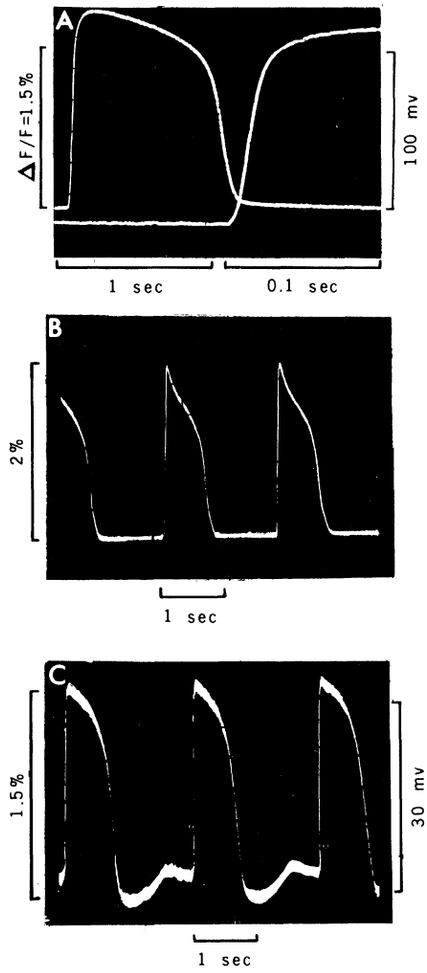


Fig. 3. Fluorometric action potentials from various regions of the frog heart. The incident beam is displaced so that the fluorescence signal from a merocyanine-stained heart is recorded from the desired region. The heart has been equilibrated in calcium-free solution for 1 hour to suppress contraction. Characteristic action potentials from (A) ventricular, (B) atrial, and (C) sinus venosus regions are indicated. The rate of rise of an electrically elicited ventricular action potential is also shown in (A). The sinus venosus cell shows the characteristically slow diastolic depolarization. The incident beam diameter was 3 mm in (A) and 1 mm in (B) and (C); 100 mv = 2.4 nw.

with a mixture of 95 percent $O_2$ and 5 percent $CO_2$ no significant effect on the viability of the tissue or the size of the signal could be demonstrated.

Thus, merocyanine 540 seems to bind to the cardiac cell membrane without any deleterious effect on contraction and is capable of monitoring the change in the myocardial membrane potential fluorometrically when excited at 540 nm. Fluorometric measurement of the optical signal combined with the use of a rapid scanning system could provide an accurate measure of the exact propagation pathway of the electrical signal in normal and diseased heart.

GUY SALAMA
MARTIN MORAD
*Departments of Physiology* and
*Biophysics, University of Pennsylvania*
*School of Medicine, Philadelphia 19174*

**References and Notes**

1. H. V. Davila, B. M. Salzberg, L. B. Cohen, *Nature (London) New Biol.* **241**, 159 (1973).
2. L. B. Cohen, B. M. Salzberg, H. V. Davila, W. N. Ross, D. Landowne, A. B. Waggoner, C. H. Wang, *J. Membr. Biol.* **19**, 1 (1974).
3. P. J. Sims, A. S. Waggoner, C. H. Wang, J. F. Hoffman, *Biochemistry* **13**, 3315 (1974).
4. J. F. Hoffman and P. C. Laris, *J. Physiol. (London)* **239**, 519 (1974).
5. B. F. Hoffman and P. F. Cranefield, *Electrophysiology of the Heart* (McGraw-Hill, New York, 1960), p. 79.
6. L. J. Kagen, *Myoglobin* (Columbia Univ. Press, New York, 1973).
7. W. N. Ross, B. M. Salzberg, L. B. Cohen, H. V. Davila, *Biophys. J.* **14**, 983 (1974).
8. L. Cohen, personal communication.
9. J. Pooler and G. S. Oxford, *J. Membr. Biol.* **12**, 339 (1973).
10. A. Arvanitaki, G. Romey, N. Chalazonitis, *C. R. Seances Soc. Biol. Paris*, **162**, 153 (1968).
11. We are grateful for the very kind help and encouragement of B. Chance, without whose financial and technical help this project would not have been possible. We are indebted to Y. Goldman for helpful suggestion and criticism. Supported by grants HL 17702, HL 15835, and GMS 12202 from the Public Health Service.

11 September 1975; revised 18 November 1975

## Color Receptor Identities of Goldfish Cones

Abstract. *Goldfish retinas were exposed to spectral lights, then incubated with nitro-blue tetrazolium chloride. Diformazan deposits revealed that five morphologically distinct cone types were segregated into three color classes: red long double and long single cones, green short double and long single cones, and blue short single and miniature short single cones.*

Receptive fields of retinal neurons must eventually be described in terms of the types and distributions of photoreceptors that provide input through synaptic contact and indirect pathways. Recent advances have been made in elucidating the color-specific cone contacts of horizontal cells (*1*) and bipolar cells (*2*) in cyprinid fish. These studies depend on correlation of cone morphology with chromatic sensitivity by microspectroscopy of visual pigments in single receptor cells. Determining the organization of color receptors in certain species, such as mammals, is substantially more difficult because of the small size of the cone outer segments and the lack of morphologically distinguishing features. Our efforts to elucidate the anatomy of goldfish color receptors were undertaken with the additional goal of establishing procedures that could be applied to species where microspectroscopy of visual pigments in single receptors is difficult.

We have been investigating the color coding of goldfish cones by a state-dependent cytochemical method in flat mounts of whole retinas in which the mosaic arrangements of cones are preserved. Metabolic events triggered in cones by photon capture can be assayed by the use of a redox probe (*3*) such as nitro-blue tetrazolium chloride (NBT). When goldfish cones are irradiated with light and exposed to NBT, they reduce NBT to NBT-diformazan (NBT-DF) faster than do nonirradiated cones (*4*). The dark blue precipitate, NBT-DF, is localized in the cone ellipsoid.

Retinas were isolated from dark-adapted animals under infrared light and mounted receptor side up on a nylon mesh support moistened with oxygenated teleost saline (*5*). Retinas were stimulated with light (*6*) for 5 minutes, or left in darkness for 5 minutes as a control, and subsequently incubated for 5 minutes in a saline-succinate-NBT medium (*7*). The retinas were fixed in 10 percent formalin–isosmotic phosphate buffer (*p*H 7.4) and examined in whole mounts. All experiments were performed at room temperature (about 22°C).

Schematic illustrations of the major types of dark-adapted goldfish cones are shown in Fig. 1a. Double (D) cones are composed of long members (LD) and short members (SD) apposed at the ellipsoid and myoid levels. Three types of single cones are found (*8*): long single cones (LS), short single cones (SS), and miniature short single cones (MSS). Arrays of D and LS cones in the "sclerad" plane and arrays of SS and MSS cones in the "vitread" plane are visible in whole mounts.

Long double and most long single cones respond to red lights by forming NBT-DF in their ellipsoids. In D cones stimulated by dim 650-nm light ($1.2 \times 10^4$ photon $sec^{-1}$ $\mu m^{-2}$) LD cones form NBT-DF, SD cones do not (Fig. 2a). In more than 10,000 D cones examined in experiments with dim 650-nm light, LD cones always responded and SD cones never did. Short single and miniature short single cones were never found to respond to dim 650-nm light. If the flux density of 650-nm

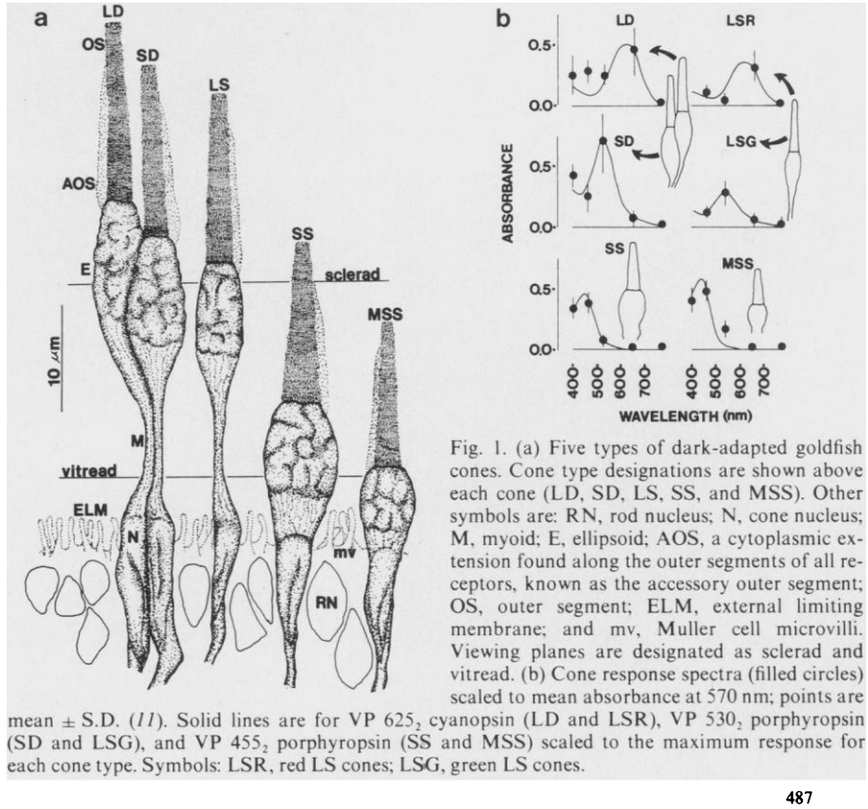


Fig. 1. (a) Five types of dark-adapted goldfish cones. Cone type designations are shown above each cone (LD, SD, LS, SS, and MSS). Other symbols are: RN, rod nucleus; N, cone nucleus; M, myoid; E, ellipsoid; AOS, a cytoplasmic extension found along the outer segments of all receptors, known as the accessory outer segment; OS, outer segment; ELM, external limiting membrane; and mv, Muller cell microvilli. Viewing planes are designated as sclerad and vitread. (b) Cone response spectra (filled circles) scaled to mean absorbance at 570 nm; points are mean ± S.D. (*11*). Solid lines are for VP $625_2$ cyanopsin (LD and LSR), VP $530_2$ porphyropsin (SD and LSG), and VP $455_2$ porphyropsin (SS and MSS) scaled to the maximum response for each cone type. Symbols: LSR, red LS cones; LSG, green LS cones.